Some aspects of the crystal-chemistry of apatites

YU LIU

Wuhan Institute of Chemical Technology, 430074-Hubei, P.R. China

AND

PAOLA COMODI

Dipartimento di Scienze della Terra, Università di Perugia, 06100-Perugia, Italia

Abstract

Twenty-four apatite (Ap) samples mainly from carbonatite and alkaline rocks were studied by electron microprobe, IR spectroscopy and X-ray powder diffraction. The crystal structures of six were refined using single crystal X-ray diffraction data to $R = 1.7$–2.5%. The generally high Si content of Ap from carbonatite and alkaline rock has been related to the presence of characteristic Si–O absorptions in IR spectra. Bands, whose intensities change with Si content, were observed at 520, 650, 930 and 1160 cm^{-1}. The IR absorption features of ν_3 CO_3 mode of Ap from carbonatite are different from those of ν_3 CO_3 mode of Ap from sedimentary rock. This phenomenon is probably due to the different effects of F and OH on the CO_3 substitution for PO_4. The structural refinements yield more information on the CO_3=PO_4 substitution, which is now supported also by the geometrical evolution of the tetrahedron with increasing CO_3 content: the tetrahedral size decreases and the angle distortion increases with C-content. It is likely that the triangular planar CO_3 group is disordered on the four faces of PO_4^{3-} tetrahedron. It was observed also that Ap from early-stage carbonatite is OH-dominant with considerable *LREE*, Si, CO_3 and negligible Mn, Fe, Mg, K, S and Cl contents. They have high Sr/Mn, Si/S and C/S ratios.

KEYWORDS: apatite, carbonatite, alkaline rocks, crystal-chemistry, carbonate.

Introduction

APATITE (Ap) is one of the most common accessory minerals in rocks of almost all genesis. It is regarded as a sensitive indicator of the genetic conditions of the host rocks. In igneous rocks, for example, the Ap composition suggests path of magma evolution, and their F–Cl–OH content has been proposed as an indicator of fugacities of volatiles in magmatic processes (Nash, 1984).

In this paper, special attention as been focused on the crystal-chemistry of same Ap samples from carbonatite where the Ap group is commonly up to 5% by volume (Hogarth, 1989). The characteristics of Ap from carbonatites have allowed us to study some substitution mechanisms not yet completely known. For example, many researchers think that CO_3 substitutes PO_4 (e.g. McClellan, 1980; Nathan 1984; Binder and Troll, 1989; McArthur, 1990) but the exact mechanism of CO_3 substitution in the Ap structure is still a matter of dispute. Through comparison of the crystal chemistry of Ap samples from carbonatites, especially from early-state carbonatites, with those from alkaline igneous pegmatitic, hydrothermal, metamorphic and sedimentary rocks, we have endeavoured to gain more information on substitution mechanisms.

Twenty-four samples from different geological environments were analysed by electron microprobe (EMPA) and by IR spectroscopy (IR). X-ray powder diffraction (XRPD) data permitted a check of the CO_3 content determined by IR spectra. Site assignments were facilitated with high precision crystal structure refinements (XRSCD) of six selected samples and the dependence of a and c lattice parameters on the chemical composition was investigated using high-precision cell constants.

Experimental procedure

Specimen details are given in Table 1. Hand samples were crushed to 140 mesh size, washed in water and dried and Ap was then separated using a Franz magnetic separator and heavy liquids. However, single crystals without impurities were

Mineralogical Magazine, December 1993, Vol. 57, pp. 709–719

Table 1 Information on the origin of the samples. The information on the origin of the samples 17-24 comes from Liu, unpublished manuscript.

Sample No.	Host rocks	Sample code	Locality	References
	Carbonatite			
1	Alvikite	A17a	Fort Portal, Uganda	Barker and Nixon, (1989).
2	Alvikite	A17b	Fort Portal, Uganda	Barker and Nixon, (1989).
3	Soevite	A16	Araxá,Minas Gerais,Brazil	Silva *et al.*, (1979).
4	Soevite	K6	Kaiserstuhl, Germany	Keller and Schleicher, (1990).
5	Soevite	K7	Kaiserstuhl, Germany	Keller and Schleicher, (1990).
6	Alvikite	A21a	Polino, Umbria, Italy	Stoppa and Lupini, (1991).
7	Alvikite	A21c	Polino, Umbria, Italy	Stoppa and Lupini, (1991).
8	Alvikitic lapillus	A3010	Vulture, Basilicata, Italy	Stoppa and Principe, pers. commun.
	Alkaline rock			
9	Melilitolite	A20	S.Venanzo, Umbria, Italy	Cundari and Ferguson, (1991).
10	Sanidinite	A22	Pitigliano, Tuscany, Italy	Turbeville, (1992).
11	Trachy-phonolite	A25	Titignano, Umbria, Italy	Stoppa and Lavecchia, (1992).
12	Trachy-phonolite	A26	Macchie, Umbria, Italy	Stoppa and Lavecchia, (1992).
13	Melilitite	A27	Cupaello, Latium, Italy	Cundari and Ferguson, (1991).
14	Tephrite	A301	Vulture, Basilicata, Italy	La Volpe and Principe, (1991).
15	Phonolite	A302	Vulture, Basilicata, Italy	La Volpe and Principe, (1991).
16	Tephrite	A309	Vulture, Basilicata, Italy	La Volpe and Principe, (1991).
17	**Nelsonite**	A3	Heishan, Hebei, China	
18	**Alkali Pegmatite**	A1	JiNing, Inner-Mongolia, China	
19	**Hydrothermal vein**	A2	Anhui,China	
20	**Metamorphic rocks**	A4	Huangmailing, Hubei, China	
21		A13	Jinping, Jiangsu, China	
22		A11	Wilberforce, Ontario, Canada	
23	**Phosphorite**	A5	Xifeng, Guizhou, China	
24		A7	Florida, USA	

carefully selected by hand. To separate Ap from carbonates, the crushed samples were doused in 1 : 1 acetic acid for about 24 hours until no bleb occurred, at which point new acid was added. Afterwards these samples were washed and dried. The samples of sedimentary Ap were enriched by flotation procedures.

IR: Powdered samples were mixed with KBr in different percentages (generally 1 : 200 with 2.5 mg of Ap; 1 : 400 with 1 mg of Ap for CO_3 determination and 1 : 50 with 4 mg of Ap for OH estimation) and pressed into pellets. The middle-IR absorption spectra were measured on a Perkin-Elmer 983G spectrophotometer (Dipartimento di Chimica, Università di Perugia, Italy). To evaluate the OH content, the pellets were dried at 110 °C. The IR quantitative method described by Featherstone *et al.* (1984) was applied to determine the CO_3 content (Table 2). Pure CO_3-free Ap (A22) was selected as standard and mixed with $BaCO_3$ in different percentages for calibration.

XRPD: Powder diffraction data of Ap were collected using a Philips PW1710 automatic diffractometer under standard conditions (Cu$K\alpha$ radiation, Ni filtered, 2θ range 3–70°). For the lattice parameter determination of the sedimentary Aps, NaF was applied as internal-standard. The lattice parameters (Table 3) were calculated with a least-squares program using the *d*-spacing of about 25 reflections. For the CO_3 determination, the experimental conditions of Schuffert *et al.* (1990) were applied and the CO_3 content was calculated using the Δ2θ angle of the (004) and (410) reflections (Table 2).

XRSCD: 6 crystals (A17a, K6, A20, A22, A302, A11) were selected for the intensity data collection. Before the collection of geometry and intensity data, the quality of the crystals was tested by Weissenberg photographs. The diffraction effects were consistent with $P6_3/m$ symmetry and no superstructure reflections were observed. The intensity data were collected on a Philips PW1100 single crystal diffractometer, using graphite-monochromatised Mo-$K\alpha$ radiation. Absorption was corrected using the semi-empirical method of North *et al.* (1968). The structure was refined in the $P6_3/m$ space group using the SHELX-76 package (Sheldrick, 1976). Anisotropic atomic displacement parameters were used for all atoms. Details of refinements and data collections are in Table 4, whereas bond-lengths and selected non-bonding lengths are in Table 5. Final atomic positions, thermal parameters and

Table 2. Representative average microprobe analyses. OH number was calculated by the charge difference in the formula. The asterisks (*) and (**) indicate chemical analysis from Liu (1993) and Stoppa and Liu (1993), respectively; na: not analysed; nc: not calculated; x-ray: determined by powder method

Sample code	A17a*	A17b	A16	K6	K7	A21a**	A21c**	A3010**	A20	A22	A25**	A26**	A27**	A301**	A302	A309**	A3	A1	A2	A4	A13	A11	A5	A7
CaO	54.99	54.29	54.11	55.20	54.55	55.55	56.85	54.80	53.04	52.89	53.03	54.85	53.76	55.11	53.74	53.00	55.98	54.35	54.72	54.98	54.46	55.32	53.49	50.57
MgO	0.22	0.18	0.01	0	0.05	0.12	0.12	0.09	0.06	0.06	0.13	0.21	0.12	0.14	0.21	0.24	0.12	0.02	0	0.01	0.02	0.03	0.19	0.33
SrO	0.32	0.33	0.77	0.71	0.57	0.26	0.60	0.27	0.52	0.19	0.56	0.33	0.49	0.36	0.73	0.67	0.08	0.71	1.18	0.17	0.03	0.17	0.11	0.18
MnO	0.06	0.07	0	0	0.07	0.03	0.07	0.03	0	0.11	0.04	0.07	0.05	0.02	0.04	0.03	0	0.05	0.04	0.26	0.09	0.02	0.02	0.01
Ce_2O_3	0.12	0.86	0.66	0.35	0.38	0.65	0.61	0.49	0.60	2.15	0.27	0.14	0.44	0.20	0.45	0.46	0.13	0.41	0.95	0	0	0.76	0.08	0.07
La_2O_3	0.05	0.23	0.37	0.23	0.16	0.48	0.60	0.19	0.27	0.85	0.16	0	0.05	0.03	0.12	0.32	0.02	0.14	0.48	0.04	0	0.37	0	0
Na_2O	na	0.19	na	na	0.15	0.17	0.14	0.16	na	0.17	na	0.12	0.10	0.16	0.14	0.15	0.04	0.15	0.06	0.05	0	0.08	0.43	0.53
P_2O_5	39.73	34.02	39.66	39.60	39.83	30.77	33.35	37.75	38.72	35.97	38.36	40.60	39.12	39.51	39.15	38.50	41.74	40.08	38.75	41.60	39.77	39.43	38.26	33.86
SiO_2	0.16	3.45	0.95	0.40	0.54	4.43	4.88	2.16	0.97	3.05	1.27	0.91	1.40	1.34	0.81	1.30	0.07	0.42	1.35	0.01	0.06	1.05	0.31	0.17
SO_3	0.08	0.46	0.02	0.09	0.28	0.38	0.51	0.45	0.06	1.64	1.05	0.87	1.07	1.10	0.73	0.92	0.12	0.43	0.86	0.11	0.15	0.59	0.55	0.52
CO_2	1.9	1.9	0.3	0.5	0.5	na	na	0.8	0	0	na	0	na	0.2	0.2	0	0	0.8	0.7	0.4	0.6	0.8	1.6	3.3
CO_{2X-ray}	1.2	1.2	0	0	0	na	na	0	0	0	na	0	na	0	na	na	0	0	0	0	0.2	0.6	2.0	7.7
F	1.36	1.21	1.05	1.99	1.50	2.05	1.83	0.83	4.93	3.42	3.91	2.69	3.03	1.24	1.99	1.50	3.19	2.76	2.56	3.58	3.80	4.27	3.40	3.06
Cl	0.15	0.10	0	0	0.10	0.04	0.07	0.15	0.03	0.07	0.13	0.12	0.08	0.27	0.76	0.46	0.10	0.27	0.17	0.01	0.01	0.06	0.02	0.03
O=F,Cl	0.60	0.53	0.44	0.84	0.65	0.87	0.79	0.38	2.09	1.46	1.68	1.16	1.30	0.58	1.01	0.73	1.36	1.22	1.12	1.51	1.60	1.81	1.43	1.29
Σ	98.54	96.76	97.46	98.23	98.03	94.06	98.84	97.79	97.11	99.11	97.23	99.75	98.41	99.10	98.06	96.82	100.23	99.37	100.70	99.71	97.42	101.15	97.03	91.34
Atoms per formula unit (for 10 cations in A site)																								
Ca	9.91	9.78	9.86	9.90	9.84	9.82	9.79	9.86	9.87	9.71	9.88	9.86	9.86	9.87	9.79	9.77	9.94	9.85	9.78	9.93	9.99	9.88	9.80	9.71
Mg	0.06	0.05	0	0	0.01	0.03	0.03	0.02	0.02	0.02	0.03	0.05	0.03	0.04	0.05	0.06	0.03	0	0	0	0	0	0.05	0.09
Sr	0.03	0.03	0.08	0.07	0.06	0.02	0.06	0.03	0.05	0.02	0.06	0.03	0.05	0.03	0.07	0.07	0.01	0.07	0.11	0.02	0	0.02	0.01	0.02
Mn	0	0.01	0	0	0.01	0	0	0	0	0.02	0	0.01	0	0	0	0	0	0	0	0.04	0.01	0	0	0
LREE	0	0.07	0.06	0.03	0.03	0.07	0.08	0.04	0.06	0.18	0.03	0.01	0.03	0.01	0.04	0.05	0.01	0.03	0.09	0	0	0.07	0	0
Na	nc	0.06	nc	nc	0.05	0.06	0.04	0.05	nc	0.05	nc	0.04	0.03	0.05	0.05	0.05	0.01	0.05	0.02	0.01	0	0.03	0.14	0.18
P	5.66	4.84	5.71	5.61	5.68	4.30	4.54	5.36	5.70	5.22	5.65	5.77	5.67	5.59	5.64	5.61	5.86	5.74	5.47	5.94	5.76	5.57	5.54	5.14
Si	0.03	0.58	0.16	0.07	0.09	0.73	0.78	0.36	0.17	0.52	0.22	0.15	0.24	0.22	0.14	0.22	0.01	0.07	0.23	0	0.01	0.18	0.05	0.03
S	0.01	0.06	0	0.01	0.04	0.05	0.06	0.06	0.01	0.21	0.14	0.11	0.14	0.14	0.09	0.12	0.01	0.05	0.11	0.01	0.02	0.07	0.07	0.07
C	0.44	0.44	0.07	0.11	0.11	nc	nc	0.18	0	0	nc	0	nc	0.05	0.05	0	0	0.18	0.16	0.09	0.14	0.18	0.37	0.81
F	0.72	0.64	0.56	1.05	0.80	1.07	0.93	0.44	2.71	1.85	2.15	1.43	1.64	0.66	1.07	0.82	1.67	1.47	1.35	1.91	2.06	2.25	1.84	1.73
Cl	0.04	0.03	0	0	0.03	0.01	0.02	0.04	0.01	0.02	0.04	0.03	0.02	0.08	0.22	0.13	0.03	0.08	0.05	0	0	0.02	0.01	0.01
OH_{cal}	1.24	1.44	1.59	1.63	1.45	1.17	0.97	1.51	0	0.10	0	0.41	0.09	1.19	0.94	1.10	0.66	0.47	0.80	0.06	0.30	0	0.31	0.78

Table 3 The lattice parameters of Ap samples. The e.s.d. are in parentheses. The asterisk (*) indicates the lattice parameters calculated with XRPD data.

Sample code	a (Å)	c (Å)	V (Å^3)	c/a
A17a	9.4027(4)	6.8859(5)	527.23	0.7323
A17b	9.4021(4)	6.8947(4)	527.83	0.7332
A16	9.4015(4)	6.8902(5)	527.42	0.7329
K6	9.3930(3)	6.8904(3)	526.48	0.7336
K7	9.4027(2)	6.8897(2)	527.52	0.7327
A3010	9.4151(7)	6.8929(12)	529.15	0.7321
A20	9.3839(7)	6.8931(8)	525.67	0.7346
A22	9.3948(3)	6.8956(4)	527.08	0.7340
A26	9.3886(3)	6.8857(4)	525.63	0.7334
A27	9.3953(5)	6.8846(6)	526.30	0.7328
A301	9.4148(6)	6.8854(6)	528.55	0.7313
A302	9.4211(3)	6.8796(3)	528.81	0.7302
A309	9.4124(2)	6.8768(3)	527.62	0.7306
A3	9.3791(4)	6.8836(5)	524.41	0.7339
A1	9.3808(4)	6.8884(4)	524.96	0.7343
A2	9.3943(5)	6.8964(5)	527.09	0.7341
A4	9.3721(3)	6.8867(4)	523.86	0.7348
A13	9.3703(4)	6.8854(4)	523.56	0.7348
A11	9.3822(4)	6.8959(5)	525.69	0.7350
A5*	9.367(2)	6.899(2)	524.23	0.7365
A7*	9.337(2)	6.896(2)	520.65	0.7386

Table 4 Details of data collection and refinement. Θ range (Mo$K\alpha$): 2-35°, ω scan, scan speed: 0.05°/sec, scan width: 1.6°.

Sample code	A17a	K6	A20	A22	A302	A11
crystal size (μm)	190x170x170	210x190x190	310x80x80	170x170x140	150x80x80	370x320x310
reflection set measured	hk±l	hk±l	hk±l	hk±l	hk±l	hkl,khl
measured reflections	1678	1658	1454	1681	1573	1780
independent reflections (I>3σ)	667	696	487	707	636	625
No. variables	46	43	41	44	47	41
R_{eq}	1.4	1.8	2.4	1.5	2.2	1.8
R%	1.7	1.8	2.4	1.7	1.9	2.5

observed and calculated structure factors are in Table 6*, Table 7* and Table 8*.

Scattering factors for neutral atoms were taken from the International Tables of X-ray Crystallography (1974). For the refinement of the Ca2 site a mixed curve with Ca, Ce and Sr was employed according to the analytical results.

At the first stage of refinement, only F was considered in the column for all samples. In samples A17a, K6, A22, A302, a peak on the Fourier difference which deviates about 0.3 Å from the F position indicates the presence of hydroxyl (Hughes *et al.*, 1989). The OH-content was modelled on the basis of the calculated value. Only in the sample A302 was Cl also considered in the anion column, because of its chemical composition (viz. 0.76% Cl).

The unit cell parameters of the refined samples and that of 13 other samples were determined accurately by the Philips LAT routine using approximately thirty reflections (Table 3). This routine takes care of possible inaccuracy of the diffractometer circles.

EMPA: All Ap samples were examined using an energy dispersive system (EDS) on the scanning electron microscope (SEM). No K, Fe, Ba, Y, heavy *REE*, Ti, As or V were detected. The same crystals used for the structural data collection and for most of the lattice parameter determinations were used for EMPA. Thirteen of the X-ray investigated samples were analysed by an ARL-SEMQ electron microprobe (WDS;

* Available on request from the editor.

Table 5 Selected bond and non-bonding lengths (Å). For the tetrahedron, also the volume (Å^3) is reported. The e.s.d. for bond lengths and non-bonding lengths are less than 0.003 Å.

Sample code	A17a	K6	A20	A22	A302	A11
Ca1-O1(x3)	2.404	2.402	2.397	2.401	2.403	2.401
-O2(x3)	2.457	2.455	2.458	2.457	2.457	2.457
-O3(x3)	2.805	2.808	2.810	2.812	2.807	2.798
<Ca1-O>	**2.555**	**2.555**	**2.555**	**2.557**	**2.556**	**2.552**
Ca2-O1	2.692	2.691	2.684	2.685	2.715	2.685
-O2	2.359	2.371	2.375	2.383	2.365	2.381
-O3(x2)	2.508	2.502	2.496	2.500	2.511	2.502
-O3'(x2)	2.347	2.350	2.353	2.352	2.347	2.355
-F	2.341	2.320	2.301	2.305	2.338	2.296
-OH	2.378	2.330	-	2.335	2.367	-
-Cl	-	-	-	-	2.590	-
<Ca2-O>	**2.460**	**2.461**	**2.460**	**2.462**	**2.466**	**2.463**
P-O1	1.534	1.536	1.542	1.540	1.536	1.536
-O2	1.536	1.539	1.544	1.544	1.540	1.540
-O3(x2)	1.531	1.533	1.536	1.539	1.531	1.536
<P-O>	**1.533**	**1.535**	**1.540**	**1.541**	**1.535**	**1.537**
V	**1.846**	**1.854**	**1.870**	**1.874**	**1.852**	**1.859**
Ca2-Ca2	**4.054**	**4.018**	**3.985**	**3.992**	**4.049**	**3.976**

C.N.R-Istituto di Mineralogia e Petrologia, Università di Modena, Italy) using a well-analysed natural Ap (Durango, Mexico) as standard for P, Ca and F, anorthite for Sr and Na, blende for S and sodalite for Cl. A synthetic-glass was also used as standard for Si, Ce and La. The acceleration voltage was 15 kV, sample current, measured on the brass, was 20 nA and the counting time was 20 sec. The other 2 samples were analysed with a CAMECA/CAMEBAX electron microprobe system (Centro Studi per i Problemi dell'Orogeno, Alpi Orientali, C.N.R., Padova, Italy). The microprobe analyses represented in Table 2 are the average of 2 or 3 representative analyses. Formulae were calculated by assuming 10 ions in the Ca sites; OH was calculated by the charge balance (Table 2).

Discussion

The $P6_3/m$ Ap structure [$A_{10}(XO_4)_6Z_2$, Nàray-Szabò (1930)] can be schematised with Ca1 and Ca2 (A cations) polyhedra forming columns around the central [001] hexad. Z ions are disposed in columns on the 6-fold screw-axes and isolated XO_4 tetrahedra connect calcium polyhedra. Extensive substitutions can occur in A cation polyhedra, XO_4 tetrahedra and Z ion columns.

A substitutions

The Ca in Ca1 and Ca2 polyhedra can be substituted by Na, K, Ag, Sr, Mg, Zn, Cd, Sc^{+3}, Y, REE^{+3}, Bi or U^{+4}, etc. (Nathan, 1984). In our samples, there is essentially no Fe, Ag, Zn, Cd, Sc, Bi, U and very little Mg. Na is low (generally <0.2 wt.% of Na_2O) even in Ap crystallised from alkali-rich magma. On the other hand, the sedimentary Aps contain relatively large amounts of Na (about 0.5 wt.% of Na_2O).

The content of $LREE_2O_3$ (Ce_2O_3 and La_2O_3) in Ap from early-stage carbonatite ranges from 0.17 to 1.21 wt.%. The SrO varies from 0.32 to 0.77 wt.% and MnO is less than 0.1 wt.%. The high Sr/Mn ratio agrees with the high Sr, low Mn characteristics of Ap from carbonatite (Hogarth, 1989). A similar feature was found in Ap from alkaline rocks. In samples from rocks other than carbonatites the $LREE_2O_3$ content varies from less than 0.1 (A4) to 3.0 wt.% (A22); SrO is highest (1.18 wt.%) in hydrothermal Ap and lowest (<0.2 wt.%) in sedimentary Ap. MnO is generally low, with the highest content (0.26 wt.%) occurring in metamorphic Ap.

Structural ordering of Sr and *REE* was studied by Hughes *et al.* (1991*a*,*b*). In the X-ray investigated Ap the <Ca1–O> and <Ca2–O> bond lengths present an irregular variation with the

Ree, Sr contents. The results of the occupancy refinements of the Ca1 and Ca2 sites show that the number of electrons in the Ca2 site is greater than that ascribed to the Ca atom alone, indicating a preference of *LREE* and Sr for this site.

XO_4 substitution

The PO_4 group can be substituted by SiO_4, SO_4, CO_3, VO_4, AsO_4, CrO_4, etc. (Nathan, 1984). In the samples under study, only Si, S and C were detectable.

In Ap from carbonatite, S is lower (0.02–0.51 wt.% SO_3) than in the Ap from alkaline rocks (generally more than 1 wt.%) whereas the SiO_2 content varies greatly (0.16–4.88 wt.%), even in similar crystals from the same hand-sample. Little work has been done to investigate the IR behaviour of the structural SiO_4 in natural Ap (Liu, 1981). We found that the presence of Si in the Ap structure can be observed in the IR spectra. In fact in the IR spectra of Si-bearing Ap, besides the absorptions of PO_4 and CO_3 ligands, there are some bands at 520 cm^{-1} and near 650, 930, 1160 cm^{-1}, whose intensities are proportional to the SiO_2 content (Fig. 1). No silicate impurity was mixed with these Aps as indicated by previous XRPD data and back-scattered electron images. Furthermore, these bands persist even though the IR measurements were repeated many times with different, carefully selected crystals. We are confident that these bands reflect Si–O vibrations in the Ap structure, and the presence of SiO_4 ligands, like CO_3 ligands, can be detected by IR spectra.

CO_3 is the most important XO_4 substituent in biological Ap and in some mineral Ap (e.g. sedimentary and carbonatite Ap). In our carbonatite Ap there is considerable CO_3 (0.3–1.9 wt.% of CO_2), whereas CO_3 is absent or negligible in Ap from alkaline rocks. The samples A21a and A21c are too small (less than 0.03 mm) to be separated for CO_3 determination. However the atomic difference in the P site indicates that up to 0.92 atom/cell of C might be present.

Although both sedimentary Ap (F-dominant) and carbonatite Ap (OH-dominant) are CO_3-bearing, there are some differences in their IR spectra: the high-frequency component of the ν_3 mode of CO_3 occurs at higher frequency in OH-dominant Ap (1458 cm^{-1}) than in F-dominant Ap (1452 cm^{-1}). Furthermore, it is more intense than the low-frequency component (1420 cm^{-1}), while in the F-dominant Ap, the opposite occurs (Fig. 2). Similar configurations were found in the IR spectra of some biological CO_3-bearing hydroxyl Ap (Elliott *et al.*, 1985).

The CO_3 content obtained by IR spectra is in accordance with that calculated using XRPD data only in sedimentary Ap. In Ap from other geneses, especially in Cl-bearing Ap, there is a great difference between the CO_3 contents determined by IR and XRPD data. The latter method is based on the *c/a* ratio, which is modified by the

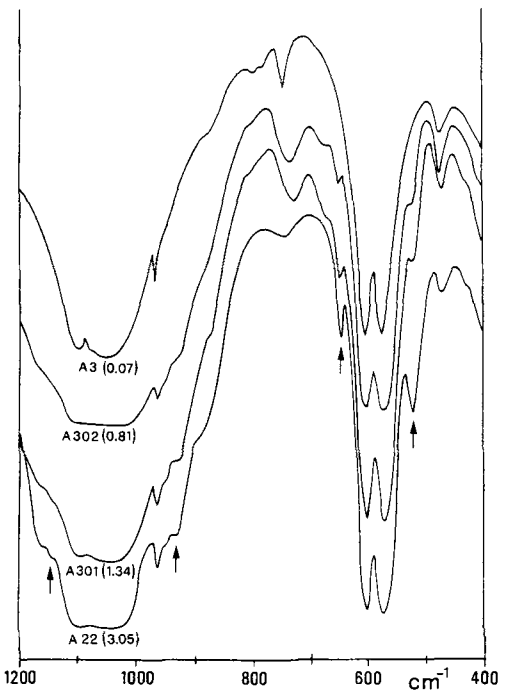

FIG. 1 Si-O IR bands of some Ap samples. The SiO_2 contents (wt.%) are reported in parentheses.

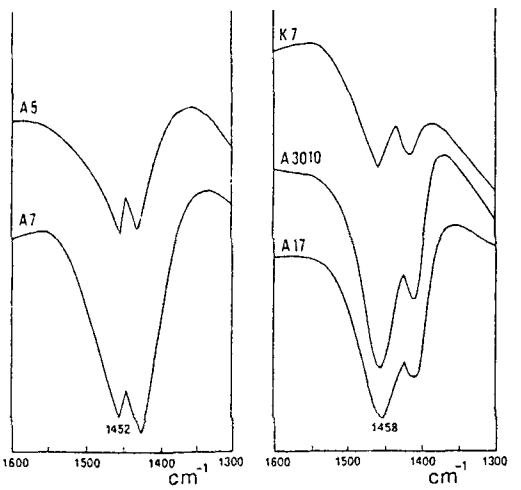

FIG. 2 Comparison of the ν_3 IR mode of CO_3 in F-dominant Ap and OH-dominant Ap.

increase of Cl and CO_3 in opposite ways (as discussed hereafter).

Only in synthetic hydroxyl-Ap prepared at high temperature and in some biological Ap, does CO_3 enter in column sites to substitute OH and F (e.g. Elliott *et al.*, 1985; Vignoles *et al.*, 1988). In all other Ap, most researchers agree that CO_3 substitutes for PO_4 (e.g. McClellan, 1980; Nathan, 1984; Binder and Troll, 1989; McArthur, 1990) although neither the structural change produced by the substitution of a tetrahedral PO_3^{3-} group with a triangular CO_3^{2-} group, nor how the charge balance is maintained, are explained. Much chemical evidence exists to support the hypothesis of CO_3/PO_4 substitution such as the high inverse correlation between the P atoms and the sum of the Si, S and C atoms (Fig. 3). On the other hand there is no crystallographic evidence to explain this substitution. The structure refinement data of our samples has allowed us to examine in detail the tetrahedral variation with C. We have observed that the mean <P–O> bond-length decreases with Si–(S+C) atoms (Fig. 4) and the bond-angle variance (Robinson *et al.*, 1971) increases with the sum of Si+S+C atoms (Fig. 5). Unfortunately the exact location of the carbonate group on the Fourier difference map is prevented by the low C-content. Moreover, the triangular CO_3 group is very likely disordered over the four tetrahedral faces.

The CO_3-bearing samples from carbonatite of Fort Portal (A17a, A17b), however, show some different crystal-chemical features: the parameter *a* is high and the *c/a* ratio is low with respect to the high CO_3 content; the diameter of the Z column is large with respect to the OH and Cl contents and the sum of X ions is far greater than 6. Such features imply that some CO_3 might enter the column. The crystal-chemistry of the Fort Portal Ap is to be discussed separately in detail in another paper (Liu, 1993).

Z substitution

Z ions lying in the columns on the 6-fold axes are generally F, OH and Cl. In the Ap investigated, only F and OH are present and the Cl-content is negligible (normally <0.15 wt.%), except in the Ap from the alkaline rocks from Vulture (up to 0.76 wt.%).

In IR spectra, the OH vibrational characteristics are represented by the frequencies and intensities of OH stretching mode (3536–3572 cm^{-1}), librational mode (670–750 cm^{-1}) and translatory mode (340–350 cm^{-1}) (Fowler, 1974). As the OH content increases, the intensities of these modes increase and the frequencies of the librational bands shift to a lower frequency. The IR features of OH, as well the calculated OH content, indicate that Ap from early-stage carbonatites is OH-dominant while Ap from alkaline rocks and of other genesis is mainly F-dominant.

Because of the strong correlation, the site-occupancy factors of F and OH anions in the Z

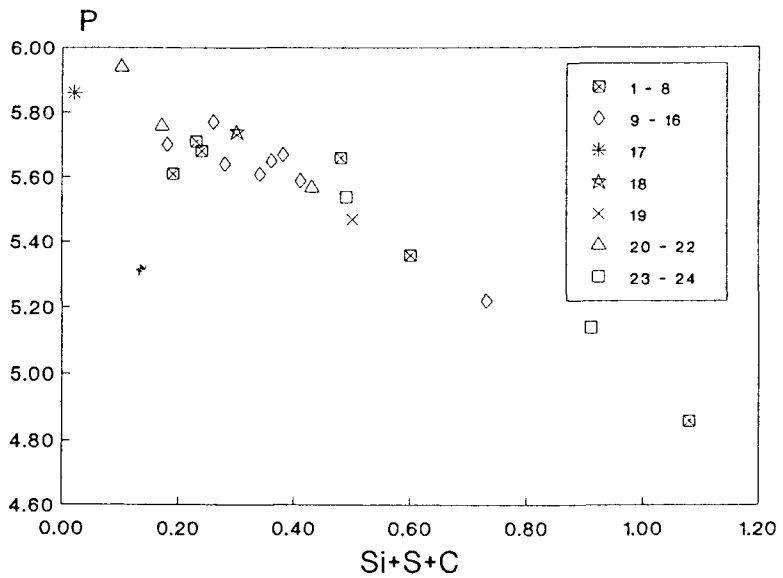

FIG. 3 Number of P *vs* the sum of Si, S, C (atom/cell). the samples A21a and A21c are not projected. The numbers in the legend represent the sample number.

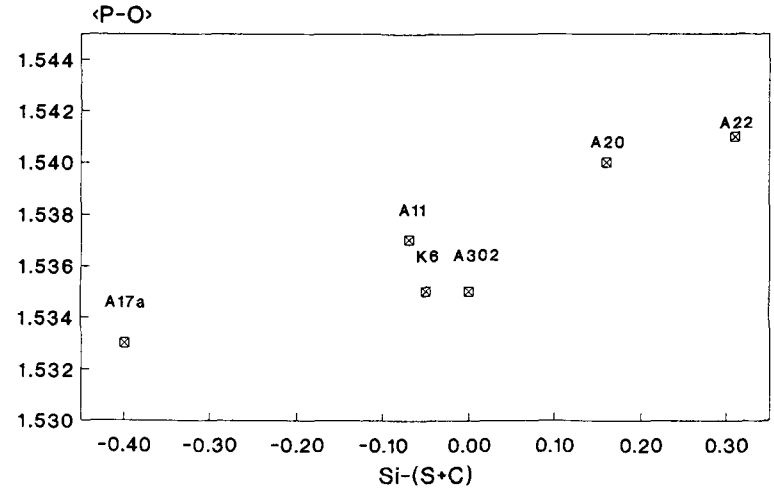

FIG. 4 Variation of <P–O> distance of tetrahedra (Å) with number of Si-(S + C) atom/cell.

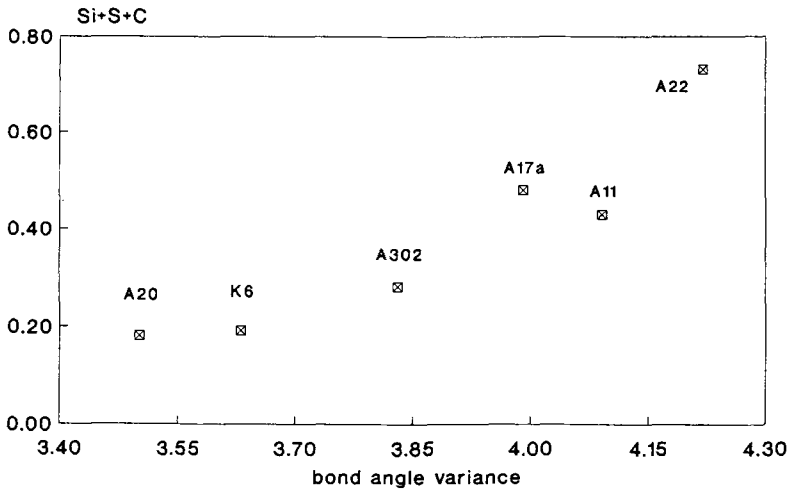

FIG. 5 Variation of the bond angle variance (deg.^{2}) with the sum of Si, S and C atom/cell.

column could not be refined simultaneously. However, the improvement of structural refinement, when the OH-content was introduced, as calculated using the analytical data (Table 2), confirms the internal consistency of these data. With the exception of the A17a sample, a direct relationship exists between the OH-content and the size of the column which is expressed by the Ca2–Ca2 distance (Table 5).

Lattice parameter variation

The accurate cell constant determination of 21 Ap samples (Table 3) allows us some considerations about the *a* and *c* parameter dependence on the chemical substitutions. OH increases both *a* and *c* parameters and leaves the *c/a* ratio almost unchanged. CO_3 and Cl are the most important factors controlling the lattice parameter ratio and they have opposite influences on it. Fig. 6 shows the *c/a* variation with C–Cl atomic difference. In F-dominant Ap, especially in sedimentary Ap, the *a* parameter is basically influenced by the CO_3 substitution for PO_4: the parameter *a* decreases whereas the *c* parameter remains unchanged with the CO_3-content. But as Cl enters the column (even in such small amounts as 0.2 atom/cell), the *a* parameter increases and

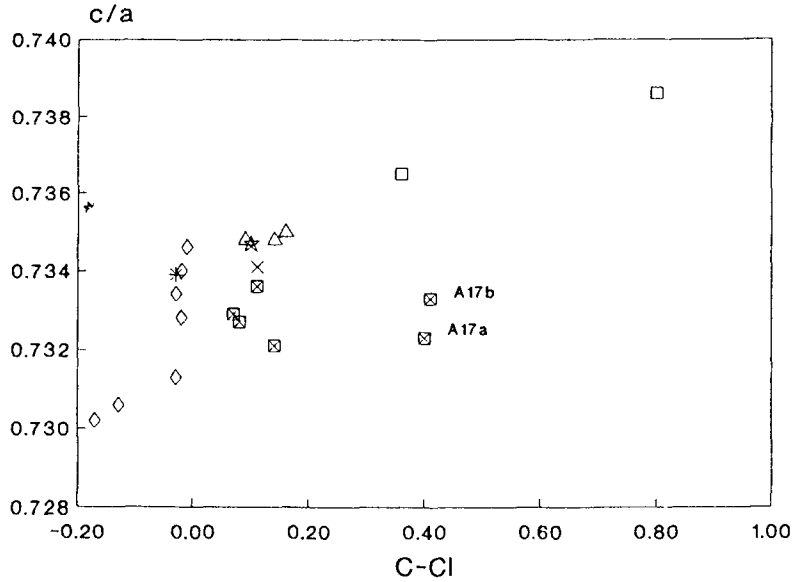

FIG. 6 The lattice parameter ratio *c/a* variation with the number of C–Cl atom/cell, symbols same as in Fig. 3.

the *c* parameter decreases greatly, resulting in a sharp decrease in the *c/a* value.

Substitution mechanisms

A direct relationship between Si and *REE* was not found, nor was a 1 : 1 Si/*REE* or Si/S atomic ratio as predicted by ideal Si/*REE*, Si/S coupled substitution. The clear direct relationship between the sums of *REE*, S and Si and Na (Fig. 7) indicates that the charge balance for the heterovalent substitution of SiO_4^{4-} for PO_4^{3-} and Na^+ for Ca^{2+} is mainly maintained by the substitution of SO_4^{2-} for PO_4^{4-} and REE^{3+} for Ca^{2+}. A combination of different substitution mechanisms both in A polyhedra and XO_4 tetrahedra, such as: $REE^{3+}+SiO_4^{4-} = Ca^{2+}+PO_4^{3-}$; $REE^{3}+Na^{+} = Ca^{2+}+Ca^{2+}$

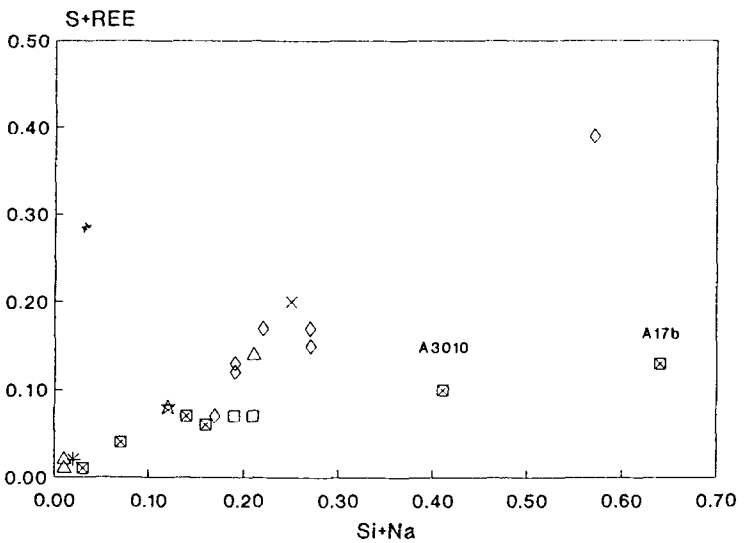

FIG. 7 The sum of *REE* and S atom/cell *vs.* the sum of Si and Na atom/cell, symbols same as in Fig. 3. The samples A21a and A21c are not projected.

(Roeder *et al.*, 1987); $SO_4^{2-} + SiO_4^{4-} = PO_4^{3-} + PO_4^{3-}$ (Hogarth, 1988), is most likely present for most of the Aps studied. Exceptions occur in the Si-, CO_3-rich Aps, (A17a, A21a, A21c and A3010), whose compositions cannot be explained completely by the above relationships. For these four Aps, it was concluded that the substitution mechanism $SiO_4^{4-} + CO_3^{2-} = PO_4^{3-} + PO_4^{3-}$ (Sommerauer and Katz-Lenhert, 1985) should be present, together with the substitution of SO_4^{2-} for PO_4^{3-}. In fact the ratio between SiO_4^{4-} and $CO_3 + SO_4$ is almost 1:1, except for the sample A17a. In this way the charge balance is ensured. Part of the carbonate may be present also as a $(CO_3OH)^{3-}$ group and the excess of negative charge could be balanced through the *LREE* entry (Sommerauer and Katz-Lenhert, op. cit.).

This mechanism has been found in Ap from carbonatite from several different localities, such as Kaiserstuhl (Sommerauer and Katz-Lenhert, 1985), Fort Portal (Barker and Nixon, 1989), Polino (Stoppa and Liu, 1993), and it seems to be a typomorphic characteristic of Ap from carbonatite.

Conclusion

On the basis of the crystal chemistry results, the following conclusions can be drawn:

The presence of Si in Ap structure can be observed in IR spectra: the intensities of the bands at 520, 650, 930 and 1160 cm^{-1} increase with Si-content.

The differences between the ν_3 IR mode of CO_3 in F-dominant and OH-dominant Ap might imply some influences of F–OH ions on the CO_3 substitution for PO_4.

The structural refinements indicate the ordering of *REE* and Sr in the Ca2 site; moreover the structural variations of tetrahedra with C-content support the hypothesis of CO_3 substitution for PO_4. The triangular CO_3 group is likely to be disordered over the four tetrahedral faces.

High Si/S, C/S, Sr/Mn and low F/OH ratios together with considerable *REE*, Si and CO_3 contents represent some characteristics of the Ap from early stage carbonatites, which allow us to distinguish them from the Aps of related alkaline rocks.

Different substitution mechanisms concerning Na, *REE*, Si, S and CO_3 for Ca and P are present in mineral Aps. Of these, the substitution mechanism $SiO_4^{4-} + (CO_3^{2-} + SO_4^{2-}) = PO_4^{3-} + PO_4^{3-}$ is a peculiar feature of the Aps from carbonatites.

Acknowledgements

We would like to thank Prof. P. F. Zanazzi for the discussion and reading of the manuscript, Dr. C. Principe, Prof. C. N. Zhong and Prof. D. S. Barker for providing the samples. Some samples and some unpublished chemical analyses were kindly made available to us by Dr. F. Stoppa. We would like to acknowledge C.N.R.—Istituto di Mineralogia e Petrologia, Modena, Italy, for the use of the ARL-SEMQ microprobe and Prof. G. Vezzalini for technical assistance. Centro Studi per i Problemi dell'Orogeno, Alpi Orientali, C.N.R., Padova, Italy, for the use of CAMECA/CAMEBAX microprobe, is also acknowledged. One of the co-authors of this paper (YL), who has been collaborating at the Dipartimento di Scienze della Terra, Perugia, Italy, under a Government Fellowship Scheme, wishes to express his special thanks to Prof. P. F. Zanazzi and to the staff of the Department for their kind help in his work. The comments of Prof. D. D. Hogarth were greatly appreciated and helped to improve the paper. This study was carried out with the financial support of C.N.R. and M.U.R.S.T. (40% funding).

References

Barker, D. S. and Nixon, P. H. (1989) High-Ca, low alkali carbonatite volcanism at Fort Portal, Uganda. *Contrib. Mineral. Petrol.*, **103**, 166–77.

Binder, G. and Troll, G. (1989) Coupled anion substitution in natural carbon-bearing apatites. Ibid., **101**, 394–401.

Cundari, A. and Ferguson, A. K. (1991) Petrogenetic relationships between melilitite and lamproite in the Roman Comagmatic Region: the lavas of S. Venanzo and Cupaello. Ibid., **107**, 343–57.

Elliott, J. C., Holcomb, D. W., and Young, R. A. (1985) Infrared determination of the degree of substitution of hydroxyl by carbonate ions in human dental enamel. *Calcif. Tissue Inter.*, **37**, 372–5.

Featherstone, J. D. B., Pearson, S., and LeGeros, R. Z. (1984) An infrared method for quantification of carbonate in carbonated apatites. *Caries Res.*, **18**, 63–6.

Fowler, B. O. (1974) Infrared studies of apatites. I. Vibrational assignments for calcium, strontium, and barium hydroxylapatites utilizing isotopic substitution. *Inorg. Chem.*, **13**, 194–207.

Hogarth, D. D. (1988) Chemical composition of fluorapatite and associated minerals from skarn near Gatineau, Quebec. *Mineral. Mag.*, **52**, 347–58.

——(1989) Pyrocholore, apatite and amphibole: distinctive minerals in carbonatite. In *Carbonatites—genesis and evolution*, (K.Bell, ed.). Unwin Hyman Ltd, London, 120–48.

Hughes, J. M., Cameron. M., and Crowley, K. D. (1989) Structural variations in natural F, OH, and Cl apatites. *Am. Mineral.*, **74**, 870–76.

——————(1991*a*) Ordering of divalent cations in the apatite structure: Crystal structure refinements of natural Mn- and Sr- bearing apatite. Ibid., **76**, 1857–62.

——— and Mariano, A. N. (1991*b*) Rare-earth-element ordering and structural variations in natural rare-earth-bearing apatites. Ibid., **76**, 1165–73.

International Tables for X-ray Crystallography (1974) Vol. 4, Kynoch Press, Birmingham, G.B.

Keller, J. and Schleicher, H. (1990) Volcanism and petrology of the Kaiserstuhl. International Volcanological Congress Mainze (FRG), Post-Conference Excursion 2B.

La Volpe, L. and Principe, C. (1991) Comments on 'Monte Vulture Volcano (Basilicata, Italy): an analysis of morphology and volcaniclastic facies' by J. E. Guest, A. M. Duncan and D. K. Chester. *Bull. Volcanol.*, **53**, 222–7.

Liu, Y. (1993) Some anomalous crystal-chemistry features of the apatite from carbonatite of Fort Portal, Uganda. (In prep.)

Liu, Y. K. (1981) Some mineralogical characters of fluorapatite in different genetic types. *Bull. Soc. Franc. Mineral. Crystall.*, **104**, 530–5.

McArthur, J. M. (1990) Fluorine-deficient apatite. *Mineral. Mag.*, **54**, 508–10.

McClellan, G. H. (1980) Mineralogy of carbonate fluorapatites. *J. Geol. Soc.*, **137**, 675–81.

Nàray-Szabò, S. (1930) The structure of apatite (CaF)-$Ca_4(PO_4)_3$. *Zeits. Kristallogr.*, **75**, 387–8.

Nash, W. P. (1984) Phosphate minerals in terrestrial igneous and metamorphic rocks. In *Phosphate Minerals*, (J. O. Nriagu and P. B. Moore, eds.). Springer-Verlag, New York, 215–41.

Nathan, Y. (1984) The mineralogy and geochemistry of phosphorites. In *Phosphate Minerals*, (J. O. Nriagu and P. B. Moore, eds.). Springer-Verlag, New York, 275–91.

North, A. C. T., Phillips, D. C., and Mathews, F. S. (1968) A semi-empirical method of absorption correction. *Acta Crystallogr.*, **A24**, 351–9.

Robinson, K., Gibbs, G. V., and Ribbe, P. H. (1971) Quadratic elongation: a quadratic measure of distortion in coordination polyhedra. *Science*, **172**, 567–70.

Roeder, P. L., McArthur, D., Ma, X. P., and Palmer, G. R. (1987) Cathodoluminescence and microprobe study of rare-earth elements in apatite. *Am. Mineral.*, **72**, 801–11.

Schuffert, J. D., Kastner, M., Emanuele, G., and Jahnke, R. A. (1990) Carbonate- ion substitution in francolite: a new equation. *Geochim. Cosmochim. Acta*, **54**, 2323–28.

Sheldrick, G. M. (1976) SHELX76, Program for crystal structure determinations. University of Cambridge, Cambridge, UK.

Silva, A. B. da, Marchetto, M., and Souza, O. M. de. (1979) Geologia do complexo carbonatitico de Araxa (Barreiro), Minas Gerais. *Mineraçao Metalurgia*, **43**, (415), 14–18.

Sommerauer, J. and Katz-Lehnert, K. (1985) A new partial substitution mechanism of CO_3^{2-}/CO_3OH^{3-} and SiO_4^{4-} for the PO_4^{3-} group in hydroxyapatite from the Kaiserstuhl alkaline complex (SW-Germany). *Contrib. Mineral. Petrol.*, **91**, 360–8.

Stoppa, F. and Lavecchia, G. (1992) Late Pleistocene ultra-alkaline magmatic activity in the Umbria-Latium region (Italy): An overview. *J. Volcan. Geoth. Res.*, **52**, (in press).

Stoppa, F. and Liu, Y. (1993) Chemical characteristics of the apatites from Italian ultra-alkaline rocks and their petrological implications. (In prep.)

——— and Lupini, L. (1991) Caratteristiche identificative di una roccia carbonatitica del pleistocene superiore affiorante presso Polino (TR-Umbria). *Studi geologici Camerti*, Vol. Speciale, 383–98.

Turbeville, B. N. (1992) Relationships between chamber margin accumulates and pore liquids: evidence from arrested *in situ* processes in ejecta, Latera caldera, Italy. *Contrib. Mineral. Petrol.*, **110**, 429–41.

Vignoles, M., Bonel. G., Holcomb, D. W., and Young, R. A. (1988) Influence of preparation conditions on the composition of type B carbonated hydroxylapatite and on the localization of the carbonate ions. *Calcif. Tissue Intern.*, **43**, 33–40.

[*Manuscript received 14 December 1992: revised 24 March 1993*]